MNRAS **000**, 1–8 (2017) Preprint 21 September 2024 Compiled using MNRAS LATEX style file v3.0

Photometric analysis of the period variation of DY Her

Zhanpei Fang,[1]★ Cristian Zanoci,[1]
[1]*Department of Physics, Stanford University, 382 Via Pueblo Mall, Stanford, CA 94305-4060, USA*

14 June 2017

ABSTRACT
DY Herculis is a high-amplitude δ Scuti star with a relatively short period and large visual magnitude variations. We conduct a series of photometric observations in the visible band of DY Her. Using differential photometry, we generate light curves which allow us to extract its period. We compute the period using maximum-likelihood estimation with Markov-Chain Monte Carlo, as well as the Lomb-Scargle method. We add four points to DY Her's O-C diagram, confirming previously reported decreases in period.

Key words: methods: observational – techniques: photometric – stars: variables: delta Scuti – stars: oscillations – stars: individual (DY Her)

1 INTRODUCTION

1.1 Delta Scuti stars

Intrinsic variable stars form a class of objects which vary in luminosity due to internal forces. The study of intrinsic variables provides valuable knowledge of the processes which occur within stars, and helps explain the diversity of stars observed in the universe.

Delta Scuti (δ Sct) stars are a class of pulsating intrinsic variable stars which lie on the classical instability strip on and near the main sequence (Breger & Pamyatnykh 1998), a region of the Hertzsprung-Russell where stars may undergo self-excited oscillations. They are Pop I short-period pulsators of spectral type A or F, with pulsation periods of less than one day, and are therefore the younger analogs of RR Lyrae stars (Baglin et al. 1973). They form the second most numerous group of pulsators in the Galaxy, after pulsating white dwarfs (Breger 1979).

Pulsations are driven by the κ-mechanism, or Eddington valve, in the He II ionization zoneBalona et al. (2015). As helium is heated it becomes more ionized, which is more opaque. At the dimmest part in the cycle, the star has highly-ionized opaque helium in its atmosphere blocking part of its light from escaping; the energy from this "blocked light" causes the helium to heat up, expand, ionize, become more transparent and therefore allow more light to pass. As more light is let through, the star appears brighter and, due to expansion, the helium begins to cool down again. Through this mechanism, helium-rich stars swell and shrink.

The pulsational period is related to the structure of the star through the pulsation equation $P\sqrt{\rho} = Q$, where P is the fundamental period, ρ is density, and Q is the pulsation constant in days (Breger 1979). As the stars evolve through the instability strip, hydrogen fuses into helium, radius increases, density decreases and period P is expected to increase.

1.2 High-amplitude δ Scuti stars

High-amplitude δ Scuti stars (HADS) are a subclass also sometimes referred to as dwarf Cepheids or AI Velorum. Boonyarak et al. (2011) defines HADS stars as variables of the A3 to F5 spectral type with pulsating periods shorter than 0.25 days and pulsation amplitudes in Johnson V band equal or larger than 0.10 magnitudes. Figure 1 shows the position of HADS stars relative to other δ Scuti stars on the Hertzsprung-Russell diagram. They pulsate radially in the fundamental or first overtone modes, and are slowly rotating (McNamara 2000). Their light curves are characterized by fast brightening and slow fading similar to classical Cepheids and RR Lyrae ab stars, with sharp maxima and broad minima.

1.3 DY Her

DY Herculis (DY Her, HIP 80903, BD+12 3028) is a HADS in the constellation Hercules, first discovered by Hoffmeister in 1935. DY Her has a relatively short period of 214.03 minutes, and its magnitude varies between 10.15 and 10.66 in the V band,[1] with radial pulsations in the fundamental or first overtone mode.

The period decrease of DY Her was first noted by Szeidl & Mahdy (1981) and confirmed by Rodríguez et al. (1995).

★ E-mail: zhanpei@stanford.edu (ZF)

[1] Data from the International Variable Star Index: https://www.aavso.org/vsx/index.php?view=detail.top&oid=14958

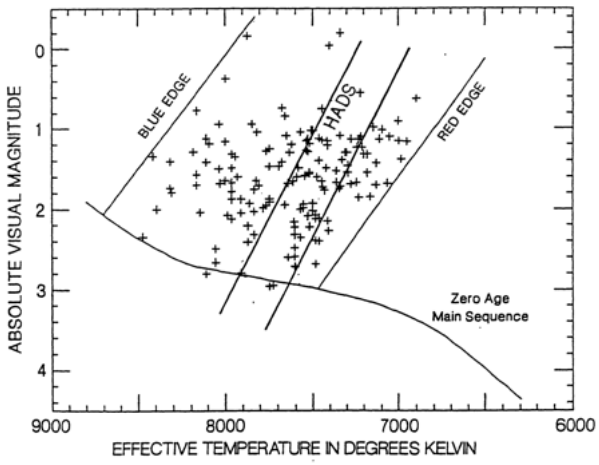

Figure 1. The position of δ Scuti variables on the instability strip of the Hertzsprung-Rusell diagram, from McNamara (2000), after Breger. Within this distribution, high-amplitude δ Scuti variables (HADS) occupy a much more restricted region, indicated by the two parallel lines just to the right of the central region between the blue and red edges of the instability strip.

Table 1. Observational properties of DY Her. Data from `http://vizier.u-strasbg.fr/viz-bin/VizieR-4`.

RA	Dec	V_{max}	V_{min}	P (days)
16h 31m 18s	+11°59′53”	10.15	10.66	0.14863

The star was studied by Derekas et al. in 2003 and 2009 (Derekas et al. 2003, 2009), and by Boonyarak and Jiang in 2007 and 2011 (Boonyarak & Jiang 2007; Boonyarak et al. 2011). These studies have shown that DY Her has a slow, continuous period decrease, contrary to evolutionary models which predict that the periods of δ Scuti variables should remain constant or increase.

Several hypotheses have been proposed to explain this behavior, namely nonlinear multimode stellar oscillations (Breger & Pamyatnykh 1998) and stellar companions (Boonyarak & Jiang 2007). Szeidl (2000) suggested that the star may be part of a binary system, and Pocs & Szeidl (2000) used the averaged O-C data and interpreted DY Her's long-term O-C diagram in terms of the light-time effect caused by a hypothetical low-mass binary companion. However, this hypothesis has been disproven by Derekas et al. (2003, 2009). Investigation of period changes in HADS stars requires more rigorous treatment than is currently available in the literature, and due to their short periods and high amplitudes, these stars are good targets for small and moderate-sized telescopes.

2 OBSERVATIONS

2.1 Data acquisition

We conduct a series of photometric observations on DY Her in order to perform differential photometry, which historically has been very effective in studying short-period variable stars. A summary of the observational properties of DY Her is presented in Table 1.

Time-series photometric observations in the V band were taken using the 16-inch telescope (16”LX200) at the Stanford Student Observatory (37.4191° N, 122.1818° W) on the night of 22 May 2017. The telescope is equatorially mounted and has a Meade Pictor 161 CCD imager focal-reduced to f/6.3. The field-of-view is $25' \times 16.7'$, and the dimensions of the CCD are 3000×2000 pixels, 0.5” each. Similarly-sized telescopes have been used in studies of DY Her in the past (Derekas et al. 2009; Boonyarak & Jiang 2007). In addition, archival photometric data from May 2016, using the same telescope, were utilized in analyses. The observational data are summarized in Table 2.

Camera control was performed using TheSky and Maxim DL software. The weather conditions were fairly clear, though some cirrus clouds were present on 22 May 2017; the May 2016 data were taken under relatively better observing conditions. This allows us to use more exposures from 2016, and results in smaller errors on our magnitudes for those three nights. During the 22 May 2017 observation, the flat-field images were observed to contain a faint dark halo at the centre; for this reason, when we took our frames we ensured that DY Her was located away from the centre.

O-C diagrams require the use of a stable and accurate clock, in order to determine the exact cycle E of the observation. The credibility of obtained astrophysical information strictly depends on the reliability of observation times and their uncertainties. For this study, time was recorded by the computer-system clock at the Stanford Student Observatory, which is not connected to the Internet; there may be an offset in zero point and possibly even variable clock rates.

2.2 Data reduction

CCD observations were reduced in Python, including bias and dark removal and flat-field corrections using sky-flat images taken during the evening twilight. For the nights when biases and darks were taken in sequences of five, we batch them together to create a master dark and master bias respectively. When calibrating our science images for those nights, we subtract the master bias and dark images that are temporally the closest to our target science image. Figure 2 displays one image of the star field, after calibrations have been made, with DY Her circled in red.

Frames were visually inspected and those which displayed obvious errors were discarded. For example, images were discarded if the shutter remained closed during the exposure, or if the point sources appeared visibly elongated due to tracking errors. For our last two observation nights, we also discarded about 15 images that were the closest to sunrise because the sunlight degraded their quality. ‘V retained’ in Table 2 is the number of exposures used in the final analysis.

UTC times given by the computer were converted to heliocentric Julian days using the `helio_jd` function in PyAstronomy. Due to the finite speed of light, the time of observation depends on the changing position of the observer in the Solar System; the heliocentric correction accounts for differences in the Earth's position with respect to the Sun.

We reduce our data using aperture photometry, with the

Table 2. Journal of observations of DY Her. Start and end times given in PDT.

Date	Bias	Dark	Flat	V	V retained	Start time	End time	Exposure time (sec)	No. reference stars
2016-05-18	10	35	10	70	70	9:48pm	12:54am	30	12
2016-05-26	7	45	10	90	87	10:06pm	1:19am	30	12
2016-05-28	80	80	10	160	143	10:07pm	4:21am	30	11
2017-05-22	15	43	10	430	346	8:56pm	3:55am	45	10

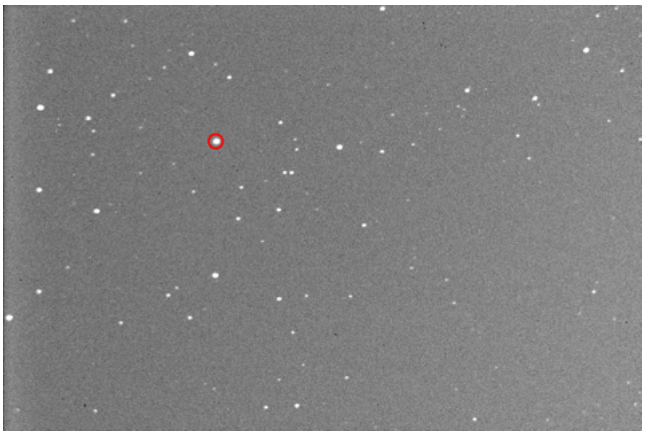

Figure 2. 45-second V-band exposure of the star field at 10:38 pm PDT on 22 May 2017. Calibration has been applied and the target star (DY Her) is circled in red.

aid of the Source Extractor program[2]. We chose an aperture radius of 6 pixels such that all stars of interest were contained well within the aperture, while ensuring that the background annulus (also of width 6 pixels) remained constant.

Differential photometry was conducted by computing the magnitude differences between DY Her and reference stars in the field. The reference stars were chosen to be those with the largest and most consistent flux throughout the night. The numbers of calibration stars used for each night are shown in Table 2. While one comparison star and one check star are typically used (Derekas et al. 2003; Baglin et al. 1973), we used this method of ensemble differential photometry in order to reduce statistical errors on our magnitudes arising from the choice of reference stars. A detailed analysis of the errors on differential magnitudes is presented in Appendix A. Magnitude errors were on the order of ±0.02, with greater errors in dusk and dawn.

Using the differential magnitudes, light curves were generated for each of the four nights of observation, as shown in Figure 3.

3 DATA ANALYSIS

There are two ways in which we assess the periodicity of DY Her: through (1) fitting the lightcurves to a function and determining times of maximum light and (2) the Lomb-Scargle method. In this section, we describe both of thee methods.

3.1 Fitting maxima

In order to create an O-C diagram, we compute the times of maximum light from the light curves. We do this by fitting functions to the lightcurve maxima, and extracting the time of maximum light from the model, which also allows us to compute the period.

The peaks were individually fit using polynomial and log normal functions. We computed a fit that minimizes the χ^2 value: $\chi^2 = \Sigma \frac{(f(x)-y)^2}{\sigma_i^2}$, where x is the time, y is the flux with associated error, and $f(x)$ is the model.

We choose to fit both a third-degree polynomial function and a log-normal distribution to the lightcurve data. Traditionally, a third- or fifth-order polynomial fit around the peak is used to determine the time of maximum light (Derekas et al. 2003, 2009). Fitting a polynomial to obtain the times of maximum light has some disadvantages. The degree of the fit is somewhat arbitrary, with many non-physical free parameters. Additionally, the polynomial fit does not use all of the available data, but only the points around the maximum.

3.2 Assessing the fit using Markov Chain Monte Carlo

Once we have models for the lightcurve maxima given the observed data, how do we evaluate the goodness of the fit? The maximum likelihood technique is implemented as follows: we derive the probability for the data given the model, treat this as a function of the model parameters (the likelihood function), and maximize the likelihood with respect to the parameters.

Markov Chain Monte Carlo (MCMC) forms a class of algorithms used to find the distribution of parameters that is consistent with a given data set, and obtaining error estimates on those parameters (Metropolis et al. 1953; Hastings 1970; Gilks et al. 1995). It is useful for sampling from probability distributions with complex relationships between parameters; for example, MCMC has been shown to perform very well on cosmological data (Tegmark et al. 2004).

MCMC performs a guided random walk through the parameter space. The Markov chain moves from one position in parameter space to the next, via a transition probability function that is chosen such that the chain's asymptotic stationary distribution equals the posterior probability on the model parameters.

In order to use this method, we must first have a sample model f for which we compute the parameter distribution.

[2] https://www.astromatic.net/software/sextractor

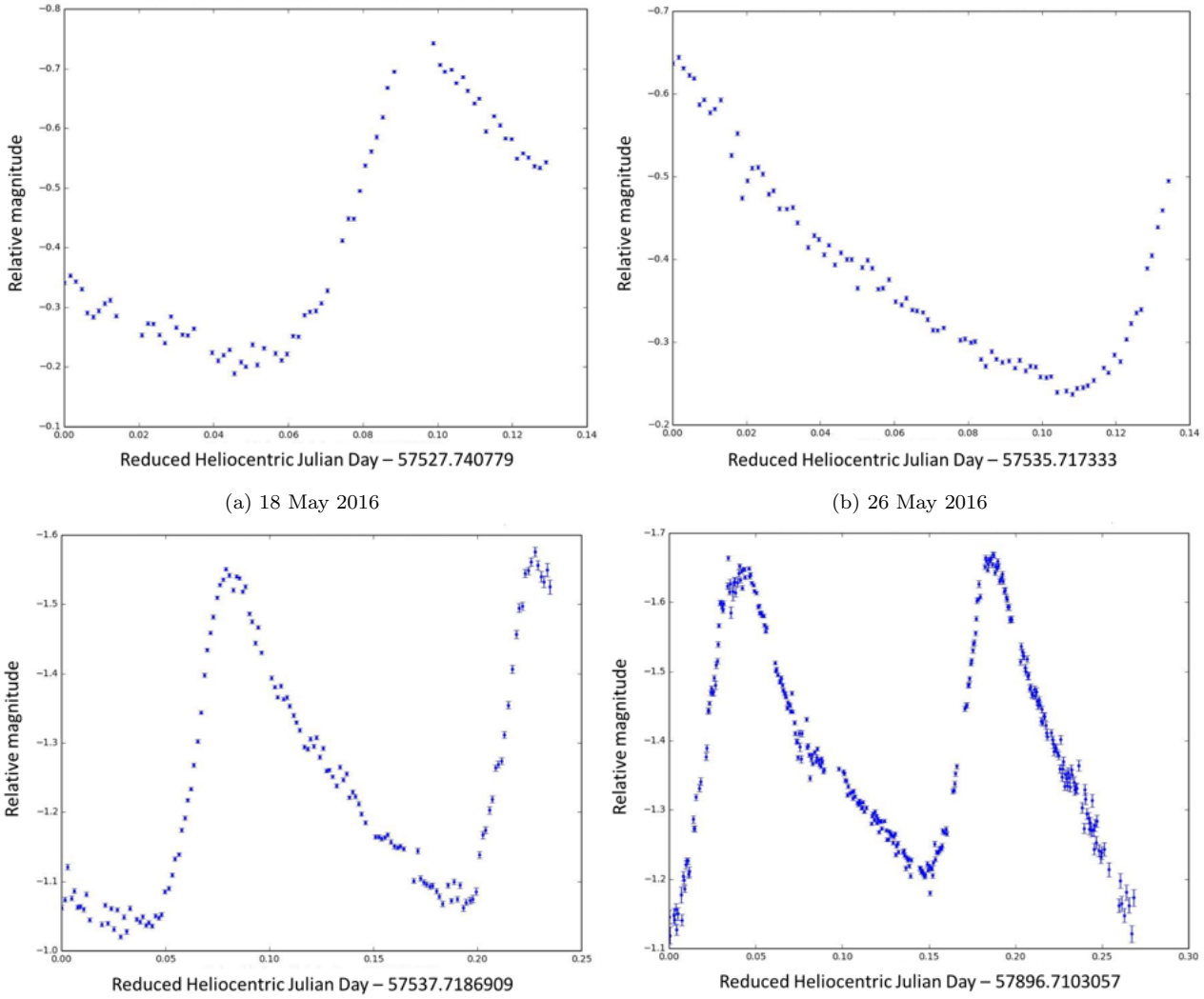

(a) 18 May 2016

(b) 26 May 2016

(c) 28 May 2016

(d) 22 May 2017

Figure 3. Light curves for each of the four nights of observation, in chronological order, with dates indicated under each plot.

Let θ represent the parameters of the model, and let (x, y, σ) denote the dataset and errors associated with y. We begin by rewriting the posterior probability on our model parameters using Bayes' theorem:

$$p(\theta|x, y, \sigma) \propto p(\theta)p(y|x, \sigma, \theta) \tag{1}$$

where we have dropped the constant term in the denominator. If we assume that the errors are Gaussian and independent, which is the case for the light curves, then we can write down the likelihood function $p(y|x, \sigma, \theta)$ as a Gaussian:

$$p(y|x, \sigma, \theta) = \prod_i \frac{1}{\sqrt{2\pi}\sigma_i} e^{-(y_i - f(x_i,\theta))^2/2\sigma_i^2} \tag{2}$$

$$= \prod_i \left(\frac{1}{\sqrt{2\pi}\sigma_i}\right) e^{-\chi^2} \propto e^{-\chi^2}. \tag{3}$$

Next, we define our prior distribution $p(\theta)$, which encodes any previous knowledge that we have about the parameters. Since the parameters of our model are arbitrary, without much physical meaning, we choose to impose a uniform, uninformative prior distribution on θ. Therefore, we end up drawing samples from the distribution $e^{-\chi^2}$, which will give us the maximum likelihood parameters and the associated errors.

In this study, we sample from a distribution of arbitrary parameters using the MCMC Hammer (`emcee`) library in Python, which implements an affine-invariant Hamiltonian MCMC (Foreman-Mackey et al. 2013). The walkers start in small distributions around the maximum likelihood values, and then quickly explore the full posterior distribution. The number of walkers should be at least an order of magnitude greater than the degrees of freedom, and we allow for a sufficiently large burn-in period to make sure that the chain is sufficiently mixed.

We first assess the third-degree polynomial fit. Figure 4 is a time series of one of the parameters in the chain; it shows the positions (parameter values) of each walker as a function of the number of steps in the chain. Figure 5 shows the plots of all generated fits for the peaks in the 22 May 2017 lightcurve, projected into the space of the observed data points; we see that the fit is very good. We then conduct

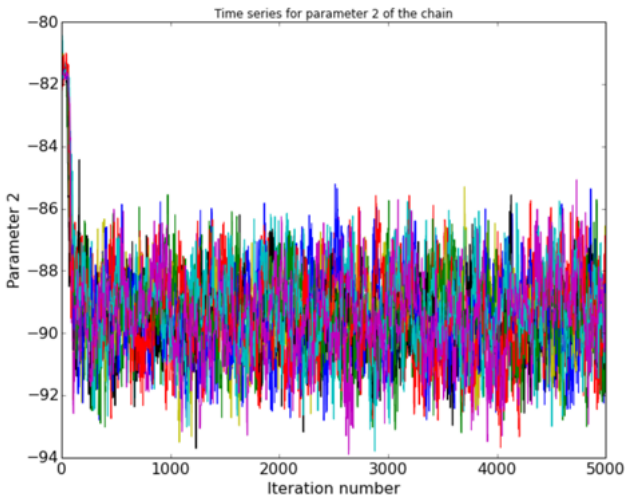

Figure 4. Example of a walk around the parameter space of a third-degree polynomial fit to the 22 May 2017 data. The burn-in time was specified to be iteration number = 1000, which is sufficient.

the same analyses on the 2017 data using the fit to a log-normal distribution; see figures 6 and 7.

3.3 The Lomb-Scargle periodogram

The Lomb-Scargle method can be used for detecting periodic variation within noisy and unevenly sampled data, and therefore can be used to calculate the period of DY Her.

The Lomb-Scargle periodogram plots a power at a set of frequencies (VanderPlas 2017), giving a measure of periodic content as a function of period. Using the data from May 2016, the periodogram (Fig 8) displays a strong peak at 214.810 minutes. Other peaks arise from linear combinations of the measurement frequency and the physical frequency; for example, in the 2017 data a peak was observed at around 48 seconds, which corresponds to a 45-second exposure with a 3-second readout time. The height of each peak is a measure of the significance level of the frequency signal.

3.4 The O-C diagram

In this paper, we construct an O-C diagram spanning 63 years in order to quantify the change in period of DY Her.

Most broadly, O-C diagrams compare the measure of an observable event and its predicted or foretold value. In astronomy, an O-C diagram is most commonly used to assess a periodic phenomenon which is believed to be subject to irregularities. In variable star studies, an O-C diagram shows the observed times of maximum light (O) minus those calculated according to an adopted ephemeris (C), plotted as a function of time. The x-axis represents time, in Julian days or the number of elapsed cycles E since the zero epoch. The y-axis is the difference between the observed time of the event (O) and the time predicted from the existing data or model of the star (C), for each event (Sterken 2005). The pattern that shows up in the O-C diagram allows us to assess the validity of a model or set of predictions; if the predicted period is even slightly off, the discrepancy will accumulate as time goes on.

For a star with a constant and correct period, points on the O-C diagram will scatter about a straight horizontal straight line, with the size of the scatter as an indication of the accuracy of the observed times of maximum. If the plot is a sloping line, the period is incorrect but constant. If it is concave-up, the events are happening later and later than expected, so the period is increasing. As discussed in section 1, this is the result expected for δ Scuti stars; by the pulsation equation, periods are expected to increase as they evolve through the instability strip and increase in radius.

A concave-down curve indicates a shortening period: the events are happening earlier and earlier than predicted. The O-C diagram for DY Her has previously been shown to be a concave-down parabola, indicating a linear decrease in period (Derekas et al. 2009). The rate of decrease of the period can be computed as the leading coefficient of a parabolic fit, as described in appendix B.

4 RESULTS

4.1 Period analysis

Table 3 shows the times of maximum light and period of DY Her calculated through the methods described above.

4.2 O-C diagram

Boonyarak & Jiang (2007) used 97 times of maximum light to conduct the analysis, and Boonyarak et al. (2011) used 103 times of maximum light. We obtain times of maximum light from Table 1 of Boonyarak et al. (2011), which was compiled from previous literature and the International Bulletin of Variable Stars (IBVS), and add the four additional points generated from our data. The times of maximum light were predicted with the following ephemeris (Derekas et al. 2003, 2009; Boonyarak & Jiang 2007) (the epoch is from the General Catalogue of Variable Stars, the period from ESA 1997):

$$HJD_{\max} = 2433439.4871 + 0.1486309 \times E \quad (4)$$

We use the observational data to update the O-C diagram, in order to assess the validity of previously reported period decreases. We add 3 or 4 points to the O-C diagram and check that they are consistent with the quadratic fit reported in the literature. Figure 9 shows the O-C diagram with our additional points.

For DY Her, the relative change has been calculated to be $\frac{1}{P}\frac{dP}{dt} = -2.96 \times 10^{-8}$ yr^{-1}, which corresponds to a decrease in period of 3.801×10^{-4} seconds per year (Derekas et al. 2009). With our data, the quadratic fit to the updated diagram looks like:

$$O-C = (-6.84025\times10^{-13})E^2+(3.74317\times10^{-7})E+4.16841\times10^{-5} \quad (5)$$

5 DISCUSSION AND CONCLUSIONS

The aim of this project was to update our knowledge of the period variations of DY Her, and potentially shed light on

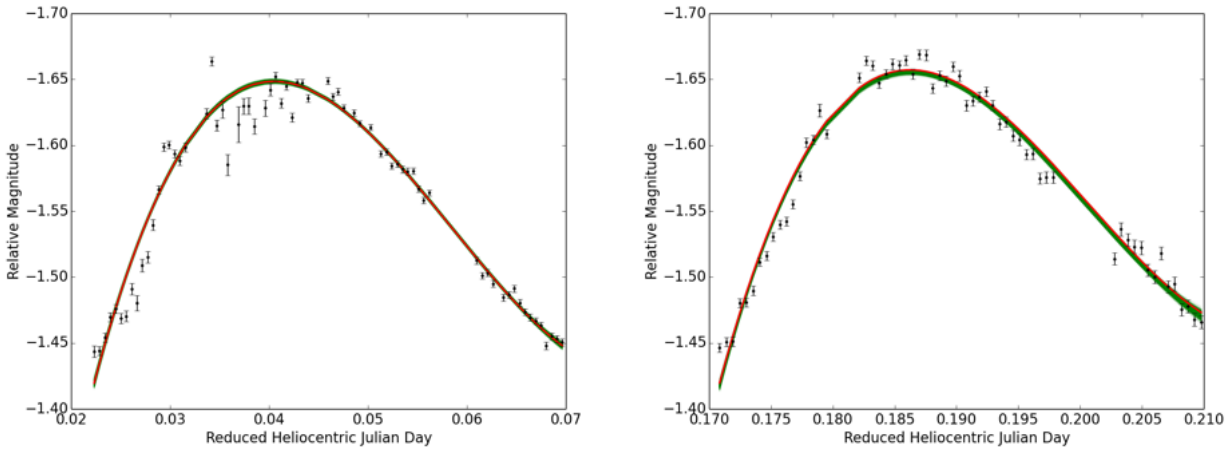

(a) Peak 1 (b) Peak 2

Figure 5. Plots of all generated third-degree polynomial fits for the peaks in the 22 May 2017 lightcurve.

Table 3. Times of maximum light and period of DY Her calculated with different methods.

Model	First time of max light t_1 (HJD_{red})	Second time of max light t_2 (HJD_{red})	P (min)
3rd-degree polynomial for 28 May 2016	$57537.79962^{+.00011}_{-.00011}$	$57537.94523^{+.00035}_{-.00030}$	$209.68960^{+.52242}_{-.45774}$
3rd-degree polynomial for 22 May 2017	$57896.75081^{+.00006}_{-.00006}$	$57896.89656^{+.00007}_{-.00007}$	$209.87287^{+.13638}_{-.13044}$
Log-normal distribution for 22 May 2017	57896.75041	57896.89912	214.14845
Lomb-Scargle for May 2016	–	–	214.05624
Lomb-Scargle for 22 May 2017	–	–	214.81083

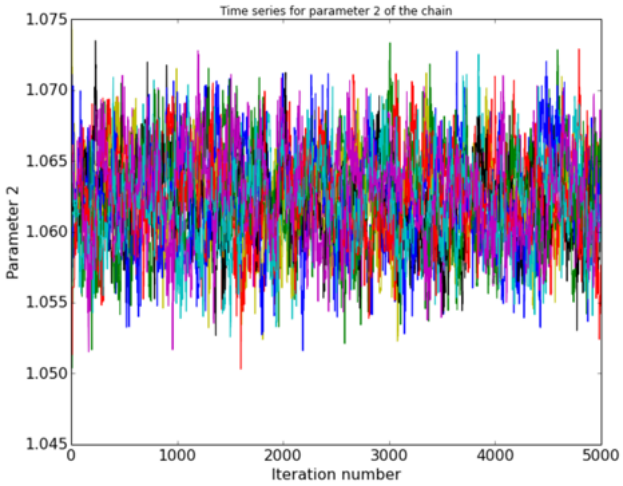

Figure 6. Example of a walk around the parameter space of a log-normal fit for 22 May 2017.

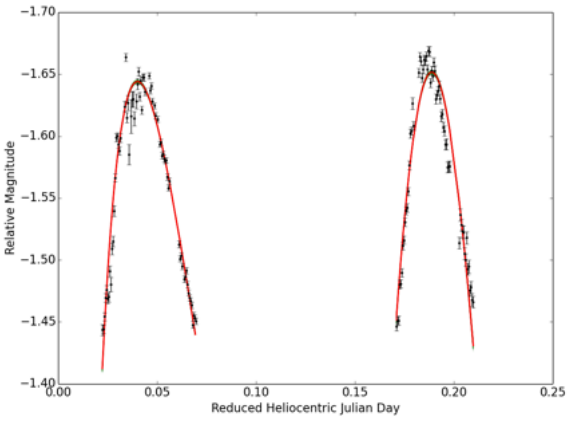

Figure 7. Plots of all generated log-normal fits for the peaks in the 22 May 2017 lightcurve.

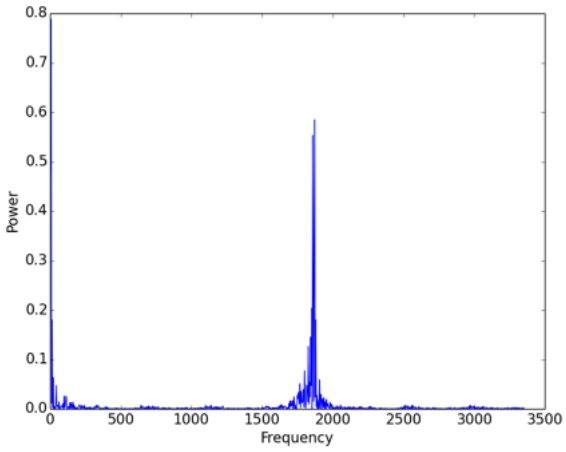

(a) Lomb-Scargle periodogram for May 2016

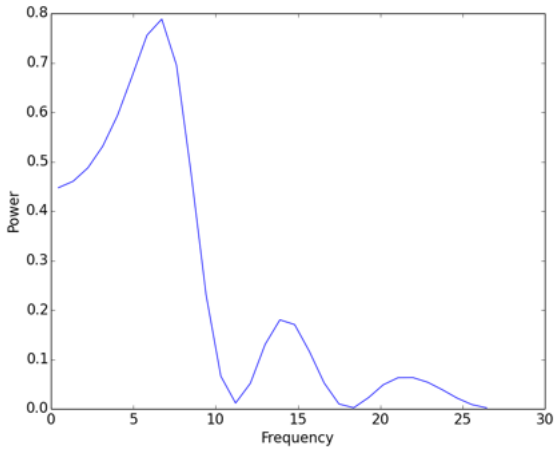

(b) The May 2016 periodogram zoomed into the peak frequency.

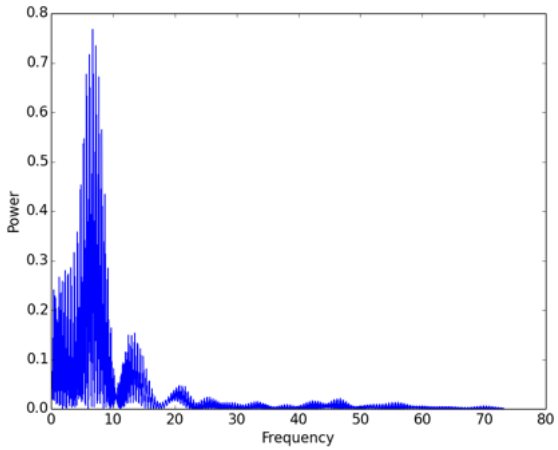

(c) Lomb-Scargle periodogram for 22 May 2017

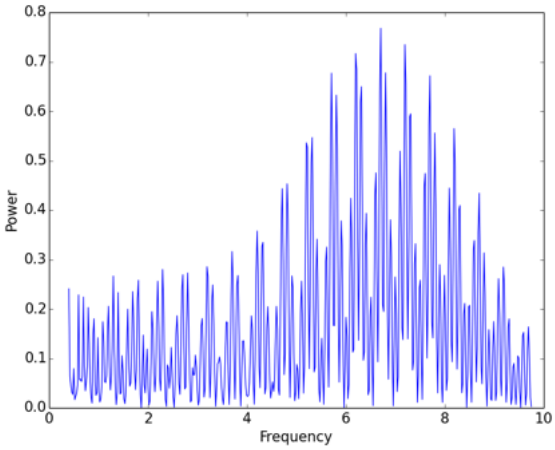

(d) The 22 May 2017 periodogram zoomed into the peak frequency.

Figure 8.

the origins of these changes. The main deliverables are an updated O-C diagram, and an estimate for relative changes in period. In this study, we have confirmed that the period of DY Her has been continuously decreasing.

There are many phenomena that can lead to period changes. Two possible causes of period changes are: an unseen binary companion, or stellar evolution. With more observations over longer time spans, we can identify real period variations caused by potential stellar evolution or binary effects.

ACKNOWLEDGEMENTS

We would like to extend our deep gratitude to the Physics 100 teaching staff – Prof. Steve Allen, Anna Ogorzalek, and Emil Noordeh – for their instruction and support throughout this research project. In addition, we thank Henry LeBrun Ingram and Tim Arthur Lann for providing observational data from May 2016.

REFERENCES

Baglin A., Breger M., Chevalier C., Hauck B., Le Contel J., Sareyan J., Valtier J., 1973, Astronomy and Astrophysics, 23, 221

Balona L. A., Daszyńska-Daszkiewicz J., Pamyatnykh A. A., 2015, MNRAS, 452, 3073

Boonyarak C., Jiang S., 2007, Astrophysics and Space Science, 310, 285

Boonyarak C., Fu J.-N., Khokhuntod P., Jiang S.-Y., 2011, Astrophysics and Space Science, 333, 125

Breger M., 1979, Publications of the Astronomical Society of the Pacific, 91, 5

Breger M., Pamyatnykh A., 1998, arXiv preprint astro-ph/9802076

Derekas A., et al., 2003, Astronomy & Astrophysics, 402, 733

Derekas A., et al., 2009, Monthly Notices of the Royal Astronomical Society, 394, 995

Foreman-Mackey D., Hogg D. W., Lang D., Goodman J., 2013, Publications of the Astronomical Society of the Pacific, 125, 306

Gilks W. R., Richardson S., Spiegelhalter D., 1995, Markov chain Monte Carlo in practice. CRC press

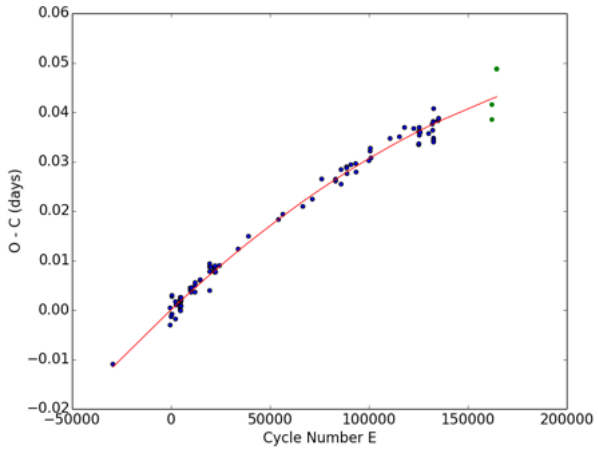

Figure 9. The updated O-C diagram for DY Her. The points in blue are from Boonyarak et al. (2011), while the green points are computed with our observational data. There are four additional points in total, though the top two points are nearly overlapping.

Hastings W. K., 1970, Biometrika, 57, 97
McNamara D., 2000, in Delta Scuti and related stars. p. 373
Metropolis N., Rosenbluth A. W., Rosenbluth M. N., Teller A. H., Teller E., 1953, The journal of chemical physics, 21, 1087
Pocs M., Szeidl B., 2000, Information Bulletin on Variable Stars, 4832
Rodríguez E., López de Coca P., Costa V., Martín S., 1995, Astronomy and Astrophysics, 299, 108
Sterken C., 2005, in The Light-Time Effect in Astrophysics: Causes and cures of the OC diagram. p. 3
Szeidl B., 2000, in Delta Scuti and Related Stars. p. 442
Szeidl B., Mahdy H. A., 1981, Communications of the Konkoly Observatory Hungary, 75, 1
Tegmark M., et al., 2004, Physical Review D, 69, 103501
VanderPlas J. T., 2017, arXiv preprint arXiv:1703.09824

APPENDIX A: ERROR ANALYSIS FOR ENSEMBLE DIFFERENTIAL PHOTOMETRY

Let m_{DY} denote the absolute magnitude of DY Her, with associated error σ_{DY}, as computed through differential photometry. Suppose we have N non-variable stars in our field of view that we intend to use as calibration stars. Let the absolute magnitudes and errors on these stars be m_i and σ_i respectively; we want to compute the differential magnitude m of DY Her using this ensemble of calibration stars, for each of our science images. First, we compute the weighted average of the magnitude of the calibration stars in the field:

$$\bar{m} = \frac{\sum_{i=1}^{N} m_i \sigma_i^{-2}}{\sum_{i=1}^{N} \sigma_i^{-2}}, \tag{A1}$$

with the associated error

$$\sigma_{\bar{m}} = \sqrt{\frac{1}{\sum_{i=1}^{N} \sigma_i^{-2}}} \tag{A2}$$

The differential magnitude for DY Her can be computed as

$$m = m_{DY} - \bar{m}. \tag{A3}$$

The error on the above quantity will then be

$$\sigma_m = \sqrt{\sigma_{DY}^2 + \sigma_{\bar{m}}^2} = \sqrt{\sigma_{DY}^2 + \frac{1}{\sum_{i=1}^{N} \sigma_i^{-2}}}. \tag{A4}$$

If, for example, all the calibration stars have the same uncertainty $\sigma_1, \cdots, \sigma_N = \sigma$, then the uncertainty on m will be given by

$$\sigma_m = \sqrt{\sigma_{DY}^2 + \frac{\sigma^2}{N}}. \tag{A5}$$

This implies that using more calibration stars will help decrease the uncertainty due to the second term above by a factor of $\sqrt{N}$, when compared to the method of using just one calibration star. Choosing multiple stars to use as reference stars reduces the error.

APPENDIX B: DERIVATION OF THE O-C FORMULA

The rate of period decrease can be determined from a quadratic fit to the curve. Sterken (2005) derives the relationship as follows: For period changes linear in time,

$$P(t) = P_0 + \frac{dP}{dt} t \tag{B1}$$

where P_0 is the period at time $t = 0$. Then the average period over the entire time interval t is

$$\bar{P} = \frac{t}{E} \tag{B2}$$

assuming that E cycles have elapsed during time t. Since the period is linear in time,

$$\bar{P} = \frac{P(t) + P_0}{2} = P_0 + \frac{1}{2}\frac{dP}{dt} t \tag{B3}$$

Suppose that we observe a time of maximum light for the star at time t. The observed time is then

$$O = t = \bar{P}E = P_0 E + \frac{1}{2}\frac{dP}{dt} tE = P_0 E + \frac{1}{2}\frac{dP}{dt}\bar{P}E^2 \tag{B4}$$

However, if the period were constant, we would predict that the time of maximum light ought to be

$$C = P_0 E \tag{B5}$$

Therefore

$$O - C = \frac{1}{2}\bar{P}\frac{dP}{dt}E^2 \tag{B6}$$

is the difference between the observed and expected times of the event. If the rate of change is zero, then the O-C diagram is a horizontal line. If the period is decreasing, then $O-C < 0$ and we would observe a concave downward parabola. The numerical value of $\frac{dP}{dt}$ is obtained through a quadratic fit; units of $\frac{dP}{dt}$ are in days per cycle, seconds for century, or seconds per year.